# Feature Selection Applied to Human Tear Film Classification

Daniel G. Villaverde[1], Beatriz Remeseiro[1], Noelia Barreira[1], Manuel G. Penedo[1]
and Antonio Mosquera [2]

[1]*Department of Computer Science, University of A Coruña, Campus de Elviña s/n, 15071 A Coruña, Spain*

[2]*Department of Electronics and Computer Science, University of Santiago de Compostela, Campus Universitario Sur, 15782 Santiago de Compostela, Spain*

Keywords: Tear Film, Dry Eye Syndrome, Color Texture Analysis, Feature Selection, Filter Methods, Machine Learning.

Abstract: Dry eye is a common disease which affects a large portion of the population and harms their routine activities. Its diagnosis and monitoring require a battery of tests, each designed for different aspects. One of these clinical tests measures the quality of the tear film and is based on its appearance, which can be observed using the Doane interferometer. The manual process done by experts consists of classifying the interferometry images into one of the five categories considered. The variability existing in these images makes necessary the use of an automatic system for supporting dry eye diagnosis. In this research, a methodology to perform this classification automatically is presented. This methodology includes a color and texture analysis of the images, and also the use of feature selection methods to reduce image processing time. The effectiveness of the proposed methodology was demonstrated since it provides unbiased results with classification errors lower than 9%. Additionally, it saves time for experts and can work in real-time for clinical purposes.

## 1 INTRODUCTION

Dry eye syndrome, resulting from an inadequate tear film, is a prevalent disease which affects a wide range of population. It affects over 14% of 65+ age group according to one US study (Moss, 2000), and over 30% of the same group in a population of Chinese subjects (Jie et al., 2008). The percentage of European people affected by dry eye is quite similar. In Germany, for example, one in four patients consulting an ophthalmologist complains of the symptoms of dry eye (Brewitt and Sistani, 2001). Many sufferers will require treatment and the potential cost is significant. Therefore, monitoring the effect of the different treatments is of great importance in order to ensure the maximum benefit to each patient (Bron, 2001).

The tear film is a thin film formed by the tear fluid over the exposed ocular surface. It was classically defined by Wolff (E.Wolff, 1954) as a multi-layer structure which consists of an outer lipid layer, an intermediate aqueous layer, and a deep mucous layer. One aspect of tear film assessment is the evaluation of the lipid superficial layer (Guillon and Guillon, 1997; Thai et al., 2004), since it plays an important role in the retention of the tear film by slowing evaporation. A deficiency of this layer may cause *evaporative dry eye syndrome*. Although this layer is transparent, interference fringes are created when light rays, reflecting off the previous surface, interfere with rays which have been reflected by the posterior surface (Freeman and Hull, 2003). In this manner, both light and dark bands of interference can be observed. The number and spacing of these bands depend on the thickness of the lipid layer and the rate at which this changes (Freeman and Hull, 2003).

The Doane tear film video interferometer (Doane, 1989) consists in a light source and an observation system which captured the appearance of the tear film using a video-based system. Using this interferometer, Thai et al. (Thai et al., 2004) measured the evaporation rate, thinning characteristics and lipid layer changes in the tear film. For this purpose, they proposed a grading system in order to classify tear film images into different categories.

Based on (Thai et al., 2004), a new grading scale composed of five categories was proposed in (Remeseiro et al., nd), since the use of a digital camera produced changes in the detail seen in the digital images. The variability in appearance of these categories resulted in a major intra- as well as inter- observer variations, and so a computer-based analysis was also presented in (Remeseiro et al., nd). This previous re-

G. Villaverde D., Remeseiro B., Barreira N., G. Penedo M. and Mosquera A..
Feature Selection Applied to Human Tear Film Classification.
DOI: 10.5220/0004809403950402
In *Proceedings of the 6th International Conference on Agents and Artificial Intelligence* (ICAART-2014), pages 395-402
ISBN: 978-989-758-015-4

search demonstrated that the interference phenomena can be characterized as color texture patterns, and so the manual process can be automated with the benefits of being faster and unaffected by subjective factors. A wide set of texture analysis techniques, color spaces and machine learning algorithms were analyzed. As a summary, the co-occurrence features method for texture extraction and the Lab color space produced the best results with maximum accuracy over 90%. Regarding the machine learning algorithms, an statistical comparison of classifiers was performed and the SVM was established as the most competitive method for the problem at hand. To the best knowledge of the authors, there are no more attempts in the literature to automatically analyze tear film images acquired with the Doane interferometer.

The problem with the approach proposed in (Remeseiro et al., nd) is that the time required to extract some of the texture features is too long for clinical purposes. Reducing processing time is a critical issue in this application, so feature selection techniques will be applied in this research in order to decrease the number of features and, as a consequence, the computational time. The proposed methodology will provide reliable results in a short period of time and so the system would be highly recommended for clinical use in dry eye diagnosis.

This paper is organized as follows: Section 2 describes the steps of the methodology, Section 3 explains the experimental study performed, Section 4 shows the results and discussion, and Section 5 includes the conclusions and future lines of research.

# 2 RESEARCH METHODOLOGY

The methodology proposed in this research is illustrated in Figure 1, and aims at improving automatic human tear film classification. First, image processing is performed in order to obtain the quantitative vectors with the texture and the color information of the images. Second, feature selection methods are applied in order to select the subset of relevant features. Then, the classification step is performed and, finally, two performance measures are computed to evaluate the effectiveness of the methodology. Next, every stage will be explained in detail.

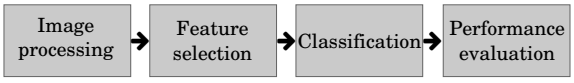


Figure 1: Steps of the research methodology.

## 2.1 Image Processing

The first step consists in processing an input image acquired with the Doane interferometer and, as a result, a quantitative vector of features is obtained. It is composed of three sub-steps: *(1)* the region of interest of an input image is extracted; *(2)* this region in RGB is converted to a specified color space; *(3)* each single channel of the transformed image is analyzed in terms of texture. As a result, a feature vector is generated. In what follows, every step will be explained in depth.

### 2.1.1 Extraction of the Region of Interest

The input images, as depicted in Figure 2(a), include an external area that does not contain useful information. Also, the most relevant information appears in the central part of the yellowish or greenish area, formed by the anterior surface of the tear film. This forces a pre-processing step aimed at extracting the *region of interest* (ROI) (Remeseiro et al., nd).

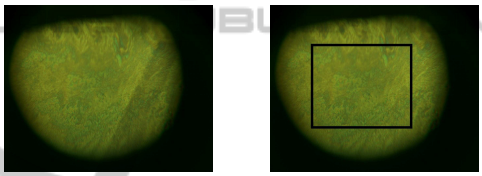

(a) (b)

Figure 2: (a) Input image in RGB. (b) Region of interest.

The relevant region of the image is characterized by green or yellow tonalities, and so only the green channel of the input image in RGB is considered. The background of the image is determined by finding those pixels whose gray level is less than a threshold:

$$th = \mu - p \times \sigma \quad (1)$$

where $\mu$ is the mean value of the gray levels of the image, $\sigma$ is its standard deviation and $p$ is a weight factor empirically determined.

Once the background is identified, the central part of the rest of the image can be located in order to extract the final ROI (see Figure 2(b)). Since some images include other irrelevant regions, such as eyelashes, the morphological operator of *erosion* (Gonzalez and Woods, 2008) is applied in order to eliminate them from further analysis. Next, a rectangle within the region identified above is selected and reduced by a pre-specified percentage. This region is likely to be free of irrelevant features and so, in most of cases, corresponds to the final ROI. However, a final step is needed in some cases: an iterative process to reduce the size of the ROI until no background areas remain.

#### 2.1.2 Color Analysis

Some categories show different color characteristics and, for this reason, images were analyzed not only in grayscale but also using the Lab color space.

- A *grayscale* image represents the color as gray levels from black to white. In order to analyze the texture over grayscale images, the three channels of the ROI in RGB are converted into a single gray channel and its texture is subsequently extracted.
- The *CIE 1976 L*a*b color space* (McLaren, 1976) is a chromatic color space appropriate for texture analysis. Using the Lab color space entails converting the three channels of the ROI in RGB to the three components of Lab. Then, each component is individually analyzed in terms of texture and the final descriptor is the concatenation of these three individual descriptors.

#### 2.1.3 Texture Analysis

Texture is used to characterize the interference patterns of the grading scale considered. As several methods for texture analysis could be applied, five popular techniques are tested in this research:

- *Butterworth filters* (Gonzalez and Woods, 2008) are frequency domain filters that have an approximately flat response in the bandpass frequency, which gradually decays in the stopband. The order of the filter defines the slope of the decay. A bank of Butterworth filters composed of 9 second order filters was used, with bandpass frequencies covering the whole frequency spectrum. The filter bank maps each input image to 9 output images, one per frequency band. Each output image was normalized separately and then a uniform histogram with non-equidistant bins was computed. Since 16-bin histograms were used, the feature vectors contain 16 components per filter.
- *Gabor filters* (Gabor, 1946) are complex exponential signals modulated by Gaussian functions. The parameters of Gabor filters define their shape, and represent their location in the spatial and frequency domains. A bank of 16 Gabor filters centered at 4 frequencies and 4 orientations was created. The filter bank maps each input image to 16 output images, one per frequency-orientation pair. Using the same idea as in Butterworth filters, the descriptor of each output image is its uniform histogram with non-equidistant bins. Since 13-bin histograms were used in grayscale and 17-bin histograms were used in Lab, the feature vectors contain 13 and 17 components per filter, respectively.
- *The discrete wavelet transform* (Mallat, 1989) generates a set of wavelets by scaling and translating a *mother wavelet*. The wavelet decomposition of an image consists of applying these wavelets horizontally and vertically, generating 4 subimages (LL, LH, HL, HH) which are then subsampled by a factor of 2. Then, the process is repeated $n-1$ times over the LL subimage, where $n$ is the number of scales. A generalized Daubechies algorithm (Daubechies, 1992) was applied as the *mother wavelet*. The descriptor of an input image is constructed by calculating the mean and the absolute average deviation of the input and LL images, and the energy of the LH, HL and HH images. Since 8 scales were used, the feature vectors contain 42 components.
- *Markov random fields* generate a texture model by expressing the gray values of each pixel in an image as a function of the gray values in a neighborhood of the pixel. In order to generate the descriptor, the directional variances proposed in (Çesmeli and Wang, 2001) were used. In this work, the neighborhood of a pixel is defined as the set of pixels within a Chebyshev distance $d$. Distances from 1 to 10 were considered and, for a distance $d$, the descriptor comprises $4d$ features.
- *Co-occurrence features analysis* (Haralick et al., 1973) is based on the computation of the conditional joint probabilities of all pairwise combinations of gray levels. For a given distance and an orientation, this method generates a set of gray level co-occurrence matrices and extracts several statistics from their elements. In general, the number of orientations and matrices for a distance $d$ is $4d$. A set of 14 statistics proposed in (Haralick et al., 1973) was computed from each co-occurrence matrix. The descriptor of an image consists of 2 properties, the mean and range across matrices of these statistics, thus obtaining a feature vector with 28 components per distance. Using the Chebyshev distance as in Markov random fields, distances from 1 to 17 were considered.

### 2.2 Feature Selection

Feature selection is a dimensionality reduction technique which consists of removing the irrelevant and redundant features in order to obtain a reduction in processing time without a degradation in performance (Guyon et al., 2006). Among the different feature selection techniques that can be found in the literature, filters are used in this research for several reasons: *(1)* they are the least time-consuming, *(2)* they rely on the general characteristics of the training data, and *(3)*

they are independent of the induction algorithm. In summary, filters are computationally simple and fast. Three filters were selected in this research based on previous works (Bolón-Canedo et al., 2013):

- *Correlation-based feature selection* (Hall, 1999) is a simple algorithm that ranks feature subsets according to a correlation based heuristic. The bias of this function is toward subsets that contain features that are highly correlated with the class and uncorrelated with each other. Irrelevant features should be ignored because they will have low correlation with the class; whilst redundant features should be discarded since they will be highly correlated with at least one of the remaining features.
- *Consistency-based filter* (Dash and Liu, 2003) evaluates the worth of a subset of features by the level of consistency in the class values when the instances are projected onto the subset of attributes. The algorithm generates a random subset $S$ from the number of features in every round. If the number of features of $S$ is lower than the best current set ($S_{best}$), the data with the features prescribed in $S$ is checked against the inconsistency criterion. If its inconsistency rate is below a prespecified one, $S$ becomes the new $S_{best}$. The inconsistency criterion specifies to what extent the dimensionally reduced data can be accepted.
- *INTERACT* (Zhao and Liu, 2007) is a subset filter based on symmetrical uncertainty (SU) and the consistency contribution (CC), which is an indicator about how significantly the elimination of a feature will affect consistency. The algorithm is made up of two parts: *(1)* the features are ranked in descending order based on their SU values, and *(2)* the features are evaluated one by one starting from the end of the ranked feature list. If the CC of a feature is lower than an established threshold, the feature is removed, otherwise it is selected.

### 2.3 Classification

Once all the features are extracted from the ROI of a single image, the obtained descriptor has to be classified into one of the considered categories. For this task, a *support vector machine* (SVM) (Burges, 1998) is trained according to the results presented in (Remeseiro et al., nd). In the aforesaid paper, an statistical analysis of machine learning algorithms was performed, and the SVM was selected as the most competitive method for the problem at hand, compared with methods such as Naive Bayes or decision trees.

### 2.4 Performance Evaluation

After the SVM is trained, the performance of the system is evaluated in terms of two different measures of relevance to the problem in question:

- The *classification error* is computed as the percentage of incorrectly classified instances.
- The *feature extraction time* is computed as the time that the texture analysis methods take to extract the selected features from a single image. Note that this does include neither the time of training a classifier nor the time of performing feature selection, since they are off-line processes.

## 3 EXPERIMENTAL STUDY

The aim of this research is to present a methodology based on color texture analysis and feature selection to classify tear film images acquired with the Doane interferometer. This methodology is tested in order to improve previous results (Remeseiro et al., nd). The materials and methods used in this research are presented in this section.

### 3.1 Data Source

In order to test the proposed methodology, a bank of images acquired from dry eye patients with average age $55 \pm 16$ was used. This dataset is publicly available in (VOPTICAL_GCU, nd). All images in this bank have been annotated by two optometrists from the Department of Life Sciences, Glasgow Caledonian University (Glasgow, UK).

The acquisition of the images was carried out with the Doane interferometer (Doane, 1989) and a digital PC-attached CMEX-1301 camera (CMEX-1301x, nd). The ImageFocus Capture and Analysis software (ImageFocus, nd) was used for image capture, and images were stored at a spatial resolution of $1280 \times 1024$ pixels in the RGB color space. Multiple images were taken for up to one minute and, due to the various artifacts associated with image capture, many of them were unsuitable for analysis. Therefore, optometrists selected only those images taken shortly after blinking, and when the eye was fully open.

The bank is composed of 106 images and includes samples from the five categories considered: 11 strong fringes, 25 coalescing strong fringes, 30 fine fringes, 26 coalescing fine fringes and 14 debris. These grades of interference patterns were defined by experimented optometrists in (Remeseiro et al., nd), and are defined as follows (see Figure 3):

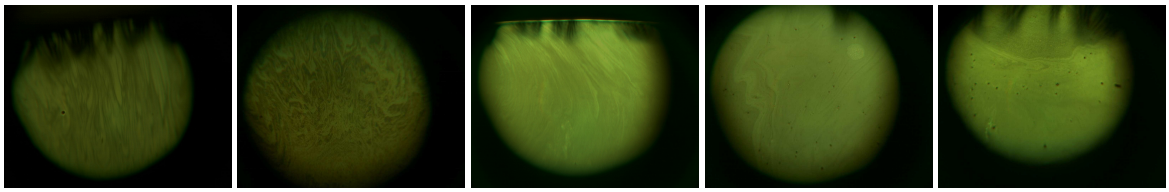

(a) (b) (c) (d) (e)

Figure 3: (a) Strong fringes. (b) Coalescing strong fringes. (c) Fine fringes. (d) Coalescing fine fringes. (e) Debris.

- *Strong fringes*. Obvious color fringes with an appearance of spreading across the cornea.
- *Coalescing strong fringes*. Obvious color fringes, but coalescing into islands of color.
- *Fine fringes*. Gray fringes with an appearance of spreading across the cornea.
- *Coalescing fine fringes*. Gray fringes, but coalescing into islands of gray.
- *Debris*. Obvious disturbances in the tear film, likely to be of varying origin.

### 3.2 Experimental Procedure

The experimental procedure is detailed as follows:

- Apply the five texture analysis methods (see Section 2.1.3) to the dataset of images using the two color spaces (see Section 2.1.2).
- Apply the three feature selection filters (see Section 2.2) to the dataset to obtain the subset of features that properly describe the problem at hand.
- Train a SVM (see Section 2.3) with radial basis kernel and automatic parameter estimation. A leave-one-out cross-validation was used, so the average error across all trials was computed.
- Evaluate the effectiveness of the proposed methodology in terms of two performance measures (see Section 2.4).

Experimentation was performed on an Intel®Core$^{TM}$i5 CPU 760 @ 2.80GHz with RAM 4 GB.

## 4 RESULTS AND DISCUSSION

The results obtained with each color space (grayscale and Lab), each texture analysis method (Butterworth filters - BF, Gabor filters - GF, the discrete wavelet transform - DWT, Markov random fields - MRF, and co-occurrence features - CF), and each feature selection filter (correlation-based feature selection - CFS, consistency-based filter - Cons, and INTERACT - INT) will be analyzed in terms of the two performance measures described above (classification error and feature extraction time). Bear in mind that the column *None* in the tables of this section shows the results when no feature selection was performed. Also, as a leave-one-out cross-validation was performed, the error, the number of features, and the time for extracting them were computed as an average value.

Table 1 shows the number of features selected by each of three feature selection filters. In average, CFS and INTERACT retain the 4.9% and 2.08% of the features, respectively; whilst consistency-based filter performed the most aggressive selection retaining only the 1.4% of the features.

Table 1: Number of features. From top to bottom, each cell contains the results corresponding to grayscale and Lab.

| | None | CFS | Cons | INT |
|---|---|---|---|---|
| | 144 | 12.52 | 8.91 | 11.43 |
| BF | 432 | 20.65 | 5.89 | 12.75 |
| | 208 | 13.92 | 7.06 | 9.68 |
| GF | 816 | 23.69 | 6.28 | 12.72 |
| | 42 | 10.95 | 5.9 | 6.18 |
| DWT | 126 | 17.67 | 6.05 | 8.80 |
| | 220 | 9 | 7.23 | 8.87 |
| MRF | 660 | 21.34 | 6.42 | 11.56 |
| | 476 | 37.64 | 4.49 | 16.83 |
| CF | 1428 | 55.9 | 4.3 | 28.75 |

Table 2 shows the test errors for all color spaces, texture analysis methods and feature selection filters after applying the SVM classifier, where the best result for each combination appears highlighted. In general, all texture analysis techniques perform quite well providing results below 16% error. Regarding the texture and color analysis without performing feature selection, it can be seen that the use of color information slightly improves the results achieved when compared to grayscale analysis since some categories contain not only morphological features, but also color features. On the other hand, all texture extraction methods perform quite well, but co-occurrence features generate the best results, closely followed by Gabor filters. Despite the fact that Markov random fields use neighborhood information, as does

co-occurrence features analysis, the Markov method does not perform as well because less information is included in the final descriptor. In essence, the combination of co-occurrence features and the INTERACT filter outperform the other methods, with the best result of 9.4% error using grayscale images. Regarding feature selection, it outperforms primal results in five out twelve pairwise combinations of color spaces and texture analysis techniques using CFS and INTERACT filters. However, the consistency-based filter produced a degradation in performance in all the combinations due to its aggressive selection.

Table 2: Mean test classification error (%). From top to bottom, each cell contains the results corresponding to grayscale and Lab.

| | None | CFS | Cons | INT |
|---|---|---|---|---|
| | **15.10** | 18.87 | 18.87 | 20.76 |
| BF | 16.88 | 21.70 | 18.87 | **15.10** |
| | **16.04** | 25.47 | 28.31 | 20.76 |
| GF | **11.32** | 16.98 | 33.02 | 17.93 |
| | 24.53 | **20.76** | 30.19 | **20.76** |
| DWT | 21.70 | **13.21** | 18.87 | 20.76 |
| | **21.70** | 22.65 | 26.42 | 23.59 |
| MRF | **15.10** | 24.53 | 23.59 | 25.47 |
| | 11.32 | 11.32 | 13.21 | **9.44** |
| CF | **11.32** | 13.21 | 16.04 | 15.10 |

The automatic grading system for human tear films should provide results to the clinicians in a very brief period of time, since waiting too long in front of a computer could be a reason for rejection of its use. In this sense, applying feature selection methods to reduce the number of input attributes and, thus, the time needed for extracting texture features can be a key step in order to improve the automatic system. In this sense, Table 3 shows the times needed for analyzing color and texture information of one single image, where the best result for each combination appears highlighted. Notice that co-occurrence features has been known to be slow and, for this reason, an optimization of the method based on (Clausi and Jernigan, 1998) was used in this research.

According to Tables 2 and 3, the effectiveness of using feature selection is demonstrated since, in most cases, the time is significantly reduced without worsening the performance. In eleven out twelve pairwise combinations, the lowest times are obtained using the most aggressive algorithm, which is consistency-based filter, and in only one case INTERACT outperforms it. The maximum processing time that would be accepted in this clinical system is around 10 or 20 seconds, and only two methods for texture analysis can be rejected for this reason (Butterworth filters and Markov random fields). Furthermore, both discrete wavelet transform and co-occurrence features analysis take less than 1 second in providing results so the system could work in real-time using these two texture analysis techniques.

Table 3: Feature extraction time (s). From top to bottom, each cell contains the results corresponding to grayscale and Lab.

| | None | CFS | Cons | INT |
|---|---|---|---|---|
| | 101.76 | 68.25 | **62.82** | 63.89 |
| BF | 305.17 | 132.96 | **47.96** | 109.60 |
| | 20.72 | 8.32 | **6.80** | 7.49 |
| GF | 62.70 | 19.89 | **8.09** | 13.38 |
| | 0.96 | 0.68 | 0.46 | **0.44** |
| DWT | 3.00 | 1.45 | **0.59** | 0.89 |
| | 74.05 | 50.82 | **33.20** | 56.98 |
| MRF | 221.72 | 104.96 | **29.29** | 67.02 |
| | 58.69 | 6.22 | **0.42** | 3.31 |
| CF | 169.22 | 20.58 | **0.34** | 8.47 |

Among all the combinations of methods, it is a very difficult task to select the best combination since two performance measures are considered. Although co-occurrence features analysis outperforms the other methods in terms of classification error and provides good results regarding feature extraction time, the Pareto front (Teich, 2001) for each alternative was computed in order to analyze the balance between error and time. In the context of multi-objective optimization, the Pareto front is defined as the set of points which are equally satisfying the constraints of the corresponding problem. Thus, selecting a solution in the Pareto front would imply to select a better solution than any outside the Pareto front. In this research, solutions are constrained to minimize both classification error and feature extraction time. Figure 4 shows the points in the Pareto front marked with a red circle. These three points correspond to: *(1)* co-occurrence features using grayscale images and INTERACT, *(2)* co-occurrence features using grayscale images and consistency-based filter, and *(3)* co-occurrence features using images in the Lab color space after applying the consistency-based filter. The selection of one of these three points will depend on if it is preferable to minimize either the error or the time for the problem at hand.

The three points in the Pareto front were analyzed in order to try to shed light on this issue. For reasons of simplicity, these three points will be referred with the numbers in Figure 4. Using the combination *(2)*, the number of features considered is approximately the same than using the combination *(3)* (4.49 and 4.3 features in average). However, the time needed for extracting these features is lower if the option *(3)* is considered (0.42 and 0.34 seconds in aver-

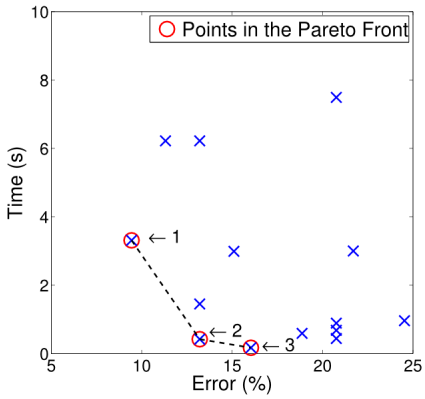


Figure 4: Pareto front for all the combinations of methods for texture extraction, color analysis and feature selection.

age). Comparing the options *(1)* and *(2)*, it can be seen that the number of features in *(1)* is almost 4 times the number of features in *(2)*, whilst the time is 8 times greater. This fact lead us to a depth analysis of the features extracted with the co-occurrence features analysis, since the time needed for obtaining its features is not homogeneous. Features are vectorized in groups of 28 related to distances and channels in the color space. Each group of 28 features corresponds with the mean and range of 14 statistics across the co-occurrence matrices. Some experiments were performed on the time the method takes to compute each of the 14 statistics. Results disclosed that computing only the $14^{th}$ statistic, which corresponds with the maximal correlation coefficient (Haralick et al., 1973), takes around 60% of the total time.

After this analysis focus on the individual features of the method proposed by Haralick, the aim here is to explore the impact of removing all the $14^{th}$ statistics. In this manner, Tables 4 and 5 show the classification error and the feature extraction time, respectively, for this experiment. From top to bottom, each cell contains the results previously obtained and the results if the $14^{th}$ statistics are excluded from each set of features. As can be seen in Table 4, the error is reduced in three out eight combinations, and maintained in two out eight combinations. Regarding Table 5, the time is reduced in seven out eight combinations and maintained in the other one. Thus, the exclusion of the $14^{th}$ statistic allows to improve the performance of the methodology. However, it is also important to remark the effectiveness of the INTERACT filter for selecting the most appropriate features since simply removing the $14^{th}$ statistics from the original set of features not only takes more time to perform feature extraction, but also produces worse results in terms of error.

Table 4: Mean test classification error (%). From top to bottom, each cell contains the results corresponding to the experiment with and without the $14^{th}$ statistic.

| | None | CFS | Cons | INT |
|---|---|---|---|---|
| CF+gray | **11.32** | **11.32** | **13.21** | 9.44 |
| | 15.10 | 14.15 | **13.21** | **8.49** |
| CF+lab | **11.32** | 13.21 | **16.04** | 15.10 |
| | **11.32** | **10.38** | 16.98 | **14.15** |

Table 5: Feature extraction time (s). From top to bottom, each cell contains the results corresponding to the experiment with and without the $14^{th}$ statistic.

| | None | CFS | Cons | INT |
|---|---|---|---|---|
| CF+gray | 58.69 | 6.22 | **0.42** | 3.31 |
| | **24.40** | **3.93** | **0.42** | **1.92** |
| CF+lab | 169.22 | 20.58 | 0.34 | 8.47 |
| | **75.59** | **5.26** | **0.31** | **2.71** |

## 5 CONCLUSIONS AND FUTURE RESEARCH

An automatic grading system to measure the quality of human tear films was developed in previous research, but it requires a too long time for extracting some texture features. This time prevents the clinical use of the system, so the aim of this work is improving previous results focus on reducing the processing time. For this task, three of the most popular feature selection filters (correlation-based feature selection, consistency-based filter and INTERACT) were tested. Results obtained with this methodology surpass the previous approach in terms of processing time and, furthermore, improves slightly the accuracy of the system.

In clinical terms, the importance of the proposed methodology lies in providing objective results in real-time, which saves time for experts who do the process by hand. Specifically, the system is able to automatically classify the images obtained using the Doane interferometer with an error lower 9% and a processing time under one second.

Future work will involve performing local analysis in order to segment one single tear film image in different categories. The motivation is that although some tear film images, from an individual subject, conformed to a single pattern, it was more common for them to be made up of a combination of different patterns. In addition, investigation of dynamic changes seen in the tear film during the inter-blink time interval would help in identifying subjects with poor tear film stability.

## ACKNOWLEDGEMENTS

This research has been partially funded by the Secretaría de Estado de Investigación of the Spanish Government and FEDER funds of the European Union through the research projects PI10/00578 and TIN2011-25476. Beatriz Remeseiro acknowledges the support of Xunta de Galicia under *Plan I2C* Grant Program.

We would also like to thank the School of Health and Life Sciences, Glasgow Caledonian University for providing us with the annotated image datasets.

## REFERENCES

Bolón-Canedo, V., Sánchez-Maroño, N., and Alonso-Betanzos, A. (2013). A review of feature selection methods on synthetic data. *Knowledge and Information Systems*, 34(3):483–519.

Brewitt, H. and Sistani, F. (2001). Dry Eye Disease: The Scale of the Problem. *Survey of Ophthalmology*, 45(2):199–202.

Bron, A. J. (2001). Diagnosis of Dry Eye. *Survey of Ophthalmology*, 45(2).

Burges, C. J. (1998). A Tutorial on Support Vector Machines for Pattern Recognition. *Data Mining and Knowledge Discovery*, 2:121–167.

Çesmeli, E. and Wang, D. (2001). Texture Segmentation Using Gaussian-Markov Random Fields and Neural Oscillator Networks. *IEEE Transactions on Neural Networks*, 12.

Clausi, D. and Jernigan, M. (1998). A Fast Method to Determine Co-occurrence Texture Features. *IEEE Transactions on Geoscience and Remote Sensing*, 36(1):298–300.

CMEX-1301x (n.d.). CMEX-1301x camera. Euromex Microscopen BV, Arnhem, The Netherlands.

Dash, M. and Liu, H. (2003). *Artificial intelligence*, 151(1-2):155–176.

Daubechies, I. (1992). *Ten Lectures on Wavelets*. SIAM, CBMS series.

Doane, M. G. (1989). An instrument for in vivo tear film interferometry. *Optometry and Vision Science*, 66(6):383–388.

E.Wolff (1954). *Anatomy of the eye and orbit (4th edition)*. H. K. Lewis and Co., London.

Freeman, M. H. and Hull, C. C. (2003). *Interference and optical films*. Butterworth Heinemann.

Gabor, D. (1946). Theory of Communication. *Journal of Institute for Electrical Engineering*, 93:429–457.

Gonzalez, R. and Woods, R. (2008). *Digital image processing*. Pearson/Prentice Hall.

Guillon, J. P. and Guillon, M. (1997). *Tearscope plus clinical hand book and tearscope plus instructions*. Keeler Ltd. Windsor, Berkshire, Keeler Inc, Broomall, PA.

Guyon, I., Gunn, S., Nikravesh, M., and Zadeh, L. (2006). *Feature Extraction: Foundations and Applications*. Springer Verlag.

Hall, M. (1999). *Ph.D dissertation, The University of Waikato*.

Haralick, R. M., Shanmugam, K., and Dinstein, I. (1973). Texture Features for Image Classification. *IEEE Transactions on Systems, Man, and Cybernetics In Systems, Man and Cybernetics*, 3:610–621.

ImageFocus (n.d.). ImageFocus Capture and Analysis software. Euromex Microscopen BV, Arnhem, The Netherlands.

Jie, Y., Xu, L., Wu, Y. Y., and Jonas, J. B. (2008). Prevalence of dry eye among adult Chinese in the Beijing Eye Study. *Eye*, 23(3):688–693.

Mallat, S. G. (1989). A theory for multiresolution signal decomposition: the wavelet representation. *IEEE Transactions on Pattern Analysis and Machine Intelligence*, 11:674–693.

McLaren, K. (1976). The development of the CIE 1976 (L*a*b) uniform colour-space and colour-difference formula. *Journal of the Society of Dyers and Colourists*, 92(9):338–341.

Moss, S. E. (2000). Prevalence of and Risk Factors for Dry Eye Syndrome. *Archives of Ophthalmology*, 118(9):1264–1268.

Remeseiro, B., Oliver, K., Tomlinson, A., Martin, E., Barreira, N., and Mosquera, A. (n.d.). Automatic grading system for human tear films. *Under review*.

Teich, J. (2001). Pareto-front exploration with uncertain objectives. In *Evolutionary multi-criterion optimization*, volume 1993, pages 314–328. Springer.

Thai, L. C., Tomlinson, A., and Doane, M. G. (2004). Effect of Contact Lens Materials on Tear Physiology. *Optometry and Vision Science*, 81(3):194–204.

VOPTICAL_GCU (n.d.). *VOPTICAL_GCU, VARPA optical dataset annotated by optometrists from the Department of Life Sciences, Glasgow Caledonian University (UK)*. [Online] Available: http://www.varpa.es/voptical_gcu.html, last access: december 2013.

Zhao, Z. and Liu, H. (2007). Searching for interacting features. pages 1156–1161.